

One-at-a-Time Designs for Estimating Elementary Effects of Simulator Experiments with Non-rectangular Input Regions

Fangfang Sun¹, Thomas J. Santner², and Angela M. Dean^{2,3}

¹*Harbin Institute of Technology, Harbin, Heilongjiang, 150001, China*

²*The Ohio State University, 1958 Neil Avenue, Columbus, OH 43210, USA*

³*University of Southampton, Southampton, SO17 1BJ, UK*

Abstract

Deterministic computer simulators are constructed from physics-, biology-, or other subject matter mathematical models. One method of identifying the influential variables among inputs to an expensive simulator is through the calculation of “elementary effects” (EEs) which measure the change in the simulator output as the value of an input changes. This paper proposes an extension of the one-at-a-time (OAT) designs introduced by Morris (1991) and modified by Campolongo, Cariboni, and Saltelli (2007) and Pujol (2009) for estimating elementary effects in rectangular input regions. The proposed method is specifically designed to be applied in non-rectangular input regions. New tools, called the $\delta \times \text{EE}$ and $x \times \text{EE}$ plots, are introduced. These plots display relationships of the EEs to gradient step lengths and input values, and provide information about the output behavior. A new criterion for selecting space-filling designs is explored.

Key words: Elementary Effects; Computer experiments; Deterministic computer simulators; Sensitivity indices; Variable selection.

1 Introduction

Global sensitivity indices based on the functional ANOVA decomposition are well-known measures of the influence of input variables on a computer simulator (or other) output when the

input space is hyper-rectangular (see, for example, Efron and Stein 1981; Sobol' 1993; Saltelli, Chan, and Scott 2000). However, although theoretically these methods can be extended to non-rectangular settings, the resulting indices are not easily interpretable. Also, as pointed out by Campolongo et al. (2007), calculation of these variance-based measures of sensitivity requires a large number of simulator runs, especially in high-dimensional applications; thus, such methods of measuring sensitivity cannot be used for simulators that take several hours or more to produce a single output. Finally, methods that estimate global sensitivity indices without huge numbers of simulator runs depend on the accuracy of an interpolating process, ordinarily a Gaussian process. In contrast, Morris (1991) proposed a method for measuring sensitivity of the output that can be used with small numbers of function evaluations and does not rely on the selection of an interpolating process. He suggested measuring the sensitivity of the output that is attributable to each input by estimating *elementary effects* (EEs), and he developed a class of *one-at-a-time* (OAT) designs for this estimation. The purpose of this paper is to propose a methodology for estimating and visualizing EEs in *non-rectangular* regions and to explore the desirability of constructing *space-filling* OAT designs.

Let $y(\mathbf{x})$ denote the deterministic computer simulator output corresponding to a vector of d inputs $\mathbf{x} = (x_1, x_2, \dots, x_d)$ and let \mathcal{X} denote the input domain of \mathbf{x} . Morris (1991) defined elementary effects through a derivative-motivated, difference quotient. He set the i^{th} elementary effect of $y(\cdot)$ at $\mathbf{x} \in \mathcal{X}$ to be

$$d_i(\mathbf{x}) = d_i(\mathbf{x}, \delta_i) = \frac{y(\mathbf{x} + \delta_i \mathbf{e}_i) - y(\mathbf{x})}{\delta_i}, \quad (1)$$

where $\mathbf{e}_i = (0, \dots, 0, 1, 0, \dots, 0)$ is the i^{th} unit vector and $\delta_i \in \mathbb{R}$ is called the (*gradient*) *step length* of the calculated effect i . Here δ_i must be selected so that $\mathbf{x} + \delta_i \mathbf{e}_i$ is also in \mathcal{X} . In principle, $d_i(\mathbf{x})$ can depend on both \mathbf{x} and δ_i but we follow the usual notational convention of suppressing the dependence on δ_i . By varying the location \mathbf{x} and value of δ_i , one can determine elementary effects $d_i(\mathbf{x})$ for input i at different starting points \mathbf{x} and different gradient step lengths, δ_i .

If $d_i(\mathbf{x})$ were rapidly computable for every input i and every vector \mathbf{x} , one could determine the distribution of the elementary effects corresponding to a given probability distribution of the inputs. Knowledge of the induced distribution of each $d_i(\cdot)$ would provide information about the impact of each input x_i on $y(\mathbf{x})$. However, if the $d_i(\cdot)$ are expensive to compute due to a slow running-simulator, Morris (1991) suggested more simply using estimates, \bar{d}_i , S_i , of the mean and standard deviation of the EEs to infer the impact of x_i on $y(\mathbf{x})$.

For simulators with hyper-rectangular input regions, which we take to be $[0, 1]^d$ for simplicity, Morris (1991) constructed OAT designs (of input runs) at which to evaluate $y(\mathbf{x})$ in order

to estimate the elementary effects for each input. For each input, his design and estimation procedure use a fixed gridding of the input region and a fixed step length $\delta_i > 0$ for input i which is taken to be a multiple of the grid spacing. Then r starting vectors $\mathbf{x}^{(k)}$, $k = 1, \dots, r$, are randomly selected from the grid in such a way that a *complete tour* within $[0, 1]^d$ is possible beginning from each $\mathbf{x}^{(k)}$. A complete tour starting at vector \mathbf{x} is a sequence of $d + 1$ input vectors determined by a sequence of random permutations $\boldsymbol{\pi} = (\pi(1), \dots, \pi(d))$ of the input labels $(1, \dots, d)$ and d randomly selected directions, $(u_1, \dots, u_d) \in \{-1, 1\}^d$. Then for $j = 1, \dots, d$, the $(j + 1)^{th}$ input vector in the tours is obtained from the j^{th} by shifting the component $x_{\pi(j)} \in [0, 1]$ to $x_{\pi(j)} + u_j \delta_j$ in such a way that $0 \leq x_{\pi(j)} + u_j \delta_j \leq 1$ and leaving all other input components fixed.

As an example with $d = 4$ inputs and a fixed $\delta_1 = \delta_2 = \delta_3 = \delta_4 = 0.2$, the five rows of

$$\begin{bmatrix} 0.4 & 0.6 & 0.6 & 0.0 \\ 0.4 & 0.4 & 0.6 & 0.0 \\ 0.2 & 0.4 & 0.6 & 0.0 \\ 0.2 & 0.4 & 0.6 & 0.2 \\ 0.2 & 0.4 & 0.4 & 0.2 \end{bmatrix}. \quad (2)$$

form a complete tour that begins at starting input vector $\mathbf{x} = (0.4, 0.6, 0.6, 0.0)$ and has successive row shifts of one component from the preceding row by an amount ± 0.2 governed by the permutation $\boldsymbol{\pi} = (2, 1, 4, 3)$ with directions $(u_1, \dots, u_4) = (-1, -1, +1, -1)$.

From a selection of r starting input vectors $\mathbf{x}^{(k)}$, $k = 1, \dots, r$, an OAT design matrix contains a total of $r \times (d + 1)$ rows, each consecutive set of $d + 1$ rows forming a complete tour. Thus, calculation can be made of r elementary effects for each input from different starting points. For example, suppose that $y(\mathbf{x}) = y(x_1, x_2, x_3, x_4)$ is the output from the simulator at input \mathbf{x} . Computing $y(\mathbf{x})$ at the first and second rows of the tour (2) produces the elementary effect $d_2(0.4, 0.6, 0.6, 0.0)$ with a signed δ_2 equal to -0.2 . Similarly the values of $y(\mathbf{x})$ evaluated at the second and third rows of the design yields the elementary effect $d_1(0.4, 0.4, 0.6, 0.0)$ with a signed δ_1 equal to -0.2 ; subsequent pairs of rows provide elementary effects $d_i(\mathbf{x})$ for the remaining inputs at different \mathbf{x} and signed δ_i values.

To describe the basic use of EEs, assume that r evaluations of each d_i are available, and let \bar{d}_i denote their sample mean and S_i denote their sample standard deviation. Morris (1991) proposed interpreting the effect of the i^{th} input on $y(\mathbf{x})$ based on \bar{d}_i and S_i as follows. An input i having a small \bar{d}_i and small S_i is non-influential (non-active); an input i having a large \bar{d}_i and small S_i has a strong linear effect on $y(\mathbf{x})$; an input i having a large S_i (and large or small \bar{d}_i) either has a non-linear effect in x_i or x_i has strong interactions with other inputs. These are easily visualized in a $\bar{d} \times S$ plot; see Figure 1 of Morris (1991).

Morris’s OAT designs for calculating elementary effects are only applicable for rectangular input regions and thus, in Section 2, we propose an alternative design algorithm, “**SeRStep**”, that can be applied to both non-rectangular and rectangular input regions. It uses *randomly selected* $\delta_i^{(k)}$ for starting point $\mathbf{x}^{(k)}$ and input i and allows selection of a *space-filling* set of starting points. Section 3 presents an example of a 6-input function with non-rectangular domain and shows that the associated estimated \bar{d}_i and S_i are consistent with theoretical expected values. A second example looks at the more complicated 20-input response function of Morris (1991), but with a modified, polygonal input region. In addition, in Section 3, we introduce new tools, $\delta \times \text{EE}$ and $x \times \text{EE}$ plots, that can give extra information about the output function.

Proposed modifications to Morris’s method include the following. Campolongo et al. (2007) suggested selection of complete tours in a OAT design by maximizing a between-tour distance measure, and Saltelli and Annoni (2010) and Campolongo, Saltelli, and Cariboni (2011) argue for radial designs which maximize distance between tours. In Section 4, we investigate the desirability of using such space-filling tours and propose an alternative distance measure which leads to more visually appealing designs. Our **SeRStep** algorithm can be modified to produce radial designs in non-rectangular regions, but these are not discussed in this paper. Pujol (2009) suggested designs based on simplexes which are non-collapsing when projected into lower-order subspaces, but analysis then requires that the model be linear at the scale of the simplexes. Campolongo et al. (2007) suggested replacing \bar{d}_i by the sample mean of the *absolute values* of the $|d_i(\mathbf{x})|$ which helps to provide information similar to the variance-based total sensitivity indices. This measure can be calculated using the EEs obtained from the **SeRStep** designs, and can be used in the plots described in place of \bar{d}_i . Section 5 provides a summary and additional areas for research.

2 The **SeRStep** Algorithm: A Flexible Method of Estimating Elementary Effects

This section describes a new algorithm, denoted **SeRStep** (**S**ecant **E**stimation with **R**andom **S**tep length δ) for constructing OAT designs that uses random gradient step lengths δ and can be used in both non-rectangular and rectangular input regions. **SeRStep** is initialized by the selection of an $r \times d$ matrix, \mathcal{S} , each of whose rows is a feasible input vector for the computer simulator. Each row of \mathcal{S} is used as the starting point (input vector) of a complete tour of the input space, where a tour consists of $d + 1$ input vectors. The outputs corresponding to

the inputs in a complete tour will be used to provide one EE (gradient), $d_i(\cdot)$, for each input i , $1 \leq i \leq d$. Thus a total of r EEs will be constructed for each input, spread over the input region. The steps in **SeRStep** are stated as follows.

Step 0: Select an $r \times d$ matrix, \mathcal{S} whose k th row provides the starting input vector $\mathbf{x}^{(k)}$ of a complete tour of the input space. For $k = 1, \dots, r$, select independent random permutations $\boldsymbol{\pi}_k = (\pi_k(1), \dots, \pi_k(d))$ of input labels $\{1, \dots, d\}$ to be associated with the r rows of \mathcal{S} . Set $k = 1$ and perform Steps 1-3.

Step 1: Select row k of \mathcal{S} and label it $\mathbf{x} = (x_1, \dots, x_d)$. Identify the associated permutation $\boldsymbol{\pi}_k = (\pi_k(1), \dots, \pi_k(d))$.

Step 2: Set $j = 1$ and perform Steps (2a)-(2d)

Step 2a: Consider input $\pi_k(j)$. Compute the *distance* from $x_{\pi_k(j)}$ to the left and right boundaries of the input region (fixing all other coordinates of \mathbf{x}); let L and R respectively, denote these distances.

Step 2b: Set the step direction for $x_{\pi_k(j)}$ to be that associated with $\max(L, R)$; that is, direction = -1 if $L > R$, and $+1$ if $L < R$

Step 2c: Randomly pick $\delta_{kj} \in [\max\{\min(L, R), 0.5 * \max(L, R)\}, \max(L, R)]$ and update $x_{\pi_k(j)}$ to $x_{\pi_k(j)} \pm \delta_{kj}$, according to the direction of the move determined in (2b).

Step 2d: If $j < d$, increment j by 1 and perform Steps (2a)-(2d)

Step 3: The sequence of $d + 1$ inputs constructed in Step 2 is a *complete tour* that begins at row k of \mathcal{S} . Use the evaluations of $y(\cdot)$ at these $d + 1$ points to determine elementary effects (1) for each input.

Step 4: If $k < r$, increment k by 1 and repeat Steps 1-3. If $k = r$, compute \bar{d}_i and S_i for each input $i = 1, \dots, d$.

To determine the r starting points in \mathcal{S} , one possibility is to use a space-filling design. If the input region is rectangular, then a maximin Latin hypercube design (LHD) scaled to the input region would be a reasonable choice for \mathcal{S} . (See Liefvendahl and Stocki 2006, for alternative space-filling designs for rectangular regions). If the input region is non-rectangular, the **ConCaD** algorithm of Draguljić, Santner, and Dean (2012) can be used to produce a space-filling and non-collapsing set, \mathcal{S} , of r starting vectors under any specified space-filling criterion. Other algorithms that produce criteria-specific space-filling sets of points are given by Trosset (1999) and Stinstra, den Hertog, Stehouwer, and Vestjens (2003).

Table 1: Expected value and standard deviation of $d_i(\mathbf{X})$ when the input vector \mathbf{X} has a uniform distribution over the region for Example 3.1

Input	$E[d_i(\mathbf{X})]$	$SD(d_i(\mathbf{X}))$
1	0.000	0.000
2	1.500	0.000
3	1.500	0.000
4	2.300	0.422
5	0.992	0.106
6	0.883	0.059

Because the construction of **SeRStep** OAT designs selects the order and direction of the tour moves *after* determining the starting points for the tours, any set of starting points can be utilized. This is in contrast to the fixed δ OAT design construction which must limit the possible starting points to those whose predetermined moves produce valid points. Thus it is simpler for **SeRStep** OAT designs to ensure that the tours start at a space-filling set of points and also more likely that the calculated EEs will explore the entire input space. The suggestion of Campolongo et al. (2007) that a well-spaced set of *tours* should be selected, and not simply a set of well-spaced starting vectors, is investigated in Section 4.

3 Examples

This section presents two examples which use the **SeRStep** algorithm to provide OAT designs and calculate EEs, as described in Section 2. The first example has six input variables and a polygonal input region for a polynomial output function whose elementary effects $d_i(\mathbf{x})$ can be calculated theoretically. The example illustrates the use of the Morris $\bar{d} \times S$ plots, and discusses extra information that can be gained from $\delta \times \text{EE}$ and $x \times \text{EE}$ plots. The second example looks at the more complicated 20-input response function of Morris (1991), but with a modified, polygonal input region. Both examples show how **SeRStep** can lead to correct identification of the important inputs and the nature of their effects on the output .

Example 3.1 Consider a 6-dimensional polygonal input region, and the output function defined by

$$y(\mathbf{x}) = 1.0 + 1.5x_2 + 1.5x_3 + .6x_4 + 1.7x_4^2 + .7x_5 + .8x_6 + .5(x_5 \times x_6),$$

for $(x_1, x_2, x_4, x_6) \in [0, 1]^4$, $x_3 \in [0, 2]$, $0 \leq x_5 \leq 2x_6/3$, and $x_5 \leq -2x_6 + 2$. This input region for $\mathbf{x} = (x_1, \dots, x_6)^\top$ can be written the form $\mathbf{Ax} \leq \mathbf{b}$ with $\mathbf{L} < \mathbf{x} < \mathbf{U}$ and the algorithm

CoNCaD (Draguljić et al. 2012) can be used to provide a non-collapsing space-filling design of starting vectors $\mathbf{x}^{(1)}, \dots, \mathbf{x}^{(r)}$. Since this is a simple output function, the EEs $d_i(\mathbf{x}^{(k)})$ can be calculated from (1) by algebra to give

1. $d_1(\mathbf{x}) \equiv 0$, because $y(\mathbf{x})$ is functionally independent of x_1 ,
2. $d_2(\mathbf{x}) = d_3(\mathbf{x}) \equiv 1.5$. The EEs of both linear terms x_2 and x_3 are non-zero constants (which is always true for additive linear terms),
3. $d_4(\mathbf{x}) = +0.6 + 1.7\delta + 3.4x_4$. The EE of the input x_4 , which has quadratic effects depends on *both* the starting value of x_4 and δ ; hence, for fixed δ , $d_4(\mathbf{x})$ will vary only with x_4 ,
4. $d_5(\mathbf{x}) = +0.7 + 0.5x_6$ and $d_6(\mathbf{x}) = +0.8 + 0.5x_5$. The EEs of the interacting x_5 and x_6 depend on the other variable.

It can be verified that the theoretical values of $E[(d_i(\mathbf{X}))]$ and $SD[(d_i(\mathbf{X}))]$ are as given in Table 1 when the input vector \mathbf{X} has a uniform distribution over the region for this example. The observed $\bar{d} \times S$ plot, obtained from a **SeRStep** OAT design starting with the $r = 15$ points selected by **CoNCaD** listed in Table 2, is shown in Figure 1. The plot clearly shows that x_1 is not active, that $y(\mathbf{x})$ has additive linear terms in x_2 and x_3 of approximately the same size ($\bar{d}_2 = \bar{d}_3 = 1.5, S_1 = S_2 = 0.0$), and that inputs $i = 4, 5, 6$ have $d_i(\mathbf{x})$ that are non-zero and vary in \mathbf{x} ($S_i > 0$). Thus $y(\mathbf{x})$ is non-linear in, or has interactions involving, x_4, x_5, x_6 . Input x_4 has the largest effect on the output.

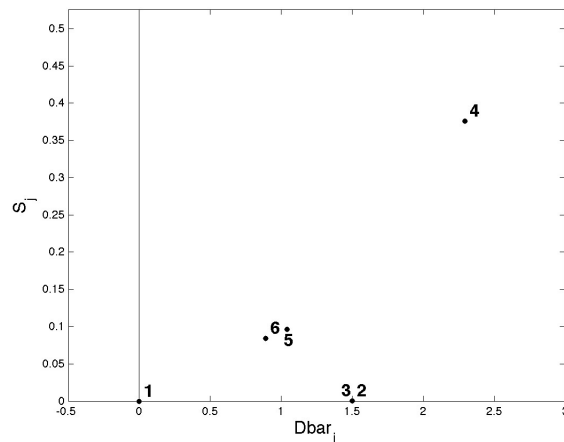


Figure 1: The $\bar{d} \times S$ plots for $y(\mathbf{x})$ in Example 3.1 based on the **SeRStep** OAT design using $r = 15$ starting points in Table 2

Table 2: The $r = 15$ starting input vectors $\mathbf{x}^{(k)}$ selected by CoNCaD for Example 3.1

x_1	x_2	x_3	x_4	x_5	x_6
1.000	0.130	1.92	0.11	0.000	0.04
0.300	0.910	0.12	0.79	0.480	0.75
0.030	0.025	0.31	0.63	0.085	0.37
0.620	0.250	1.46	0.96	0.025	0.98
0.520	0.810	2.00	0.51	0.325	0.49
0.340	0.520	0.66	0.04	0.255	0.87
0.120	1.000	0.98	0.37	0.050	0.08
0.860	0.870	0.00	1.00	0.180	0.28
0.765	0.080	0.42	0.74	0.295	0.62
0.250	0.210	1.78	0.30	0.130	0.21
0.060	0.350	1.08	0.84	0.415	0.67
0.980	0.170	1.85	0.17	0.370	0.81
0.910	0.660	0.60	0.23	0.460	0.70
0.670	0.960	1.16	0.91	0.010	0.55
0.960	0.430	1.28	0.59	0.195	0.32

For each input $i = 1, \dots, 6$, the association between the EEs, $d_i(\mathbf{x}^{(k)})$, and the $\delta_i^{(k)}$ can provide supplementary information beyond that of the $\bar{d} \times S$ plot. Figure 2 shows the $\delta_i^{(k)} \times d_i(\mathbf{x}^{(k)})$ plots for inputs $i = 1, 2, 3$ and, as expected, the EEs are constant no matter the gradient step length. The first column of Figure 3 shows the equivalent information for inputs $i = 4, 5, 6$ for this example. As in Figure 1, it is clear from Figure 3 that the most active input is input 4 (with $d_4(\mathbf{x}^{(k)})$ ranging between 1.49 and 3.09), but the $\delta \times d_4$ plot shows that, when the gradient step length $\delta_4^{(k)}$ is approximately 0.5, there are many different values for $d_4(\mathbf{x}^{(k)})$. This spread of values at fixed δ would be expected from taking a step length of δ in the x_4 direction from different starting points if the response is a non-linear function of the input. The $x_4^{(k)} \times d_4(\mathbf{x}^{(k)})$ plot indicates the strong dependence of d_4 on x_4 that would

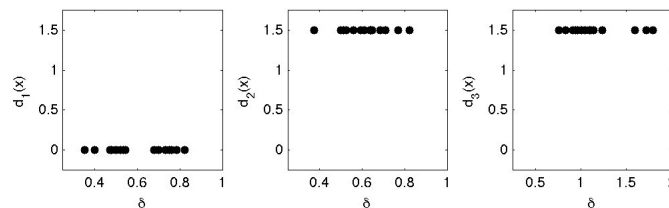


Figure 2: The $\delta_i^{(k)} \times d_i(\mathbf{x}^{(k)})$ plots for inputs $i = 1, 2, 3$ in Example 3.1 based on the SerStep OAT design using the $r = 15$ starting points \mathbf{x}_k in Table 2.

be expected for a quadratic response in x_4 . The plots in rows 2 and 3 of Figure 3 also show some variation, but the variation is much smaller (with $d_5(\mathbf{x}^{(k)})$ and $d_6(\mathbf{x}^{(k)})$ ranging between 0.8 and 1.2). The $\delta \times d_5(\mathbf{x}^{(k)})$ and $\delta \times d_6(\mathbf{x}^{(k)})$ plots seem to show some pattern but this is explained by the strong interaction between inputs 5 and 6 which is very apparent from the $x_6^{(k)} \times d_5(\mathbf{x}^{(k)})$ and $x_5^{(k)} \times d_6(\mathbf{x}^{(k)})$ plots. The random scatter in the $x_5^{(k)} \times d_4(\mathbf{x}^{(k)})$ and $x_4^{(k)} \times d_5(\mathbf{x}^{(k)})$ plots indicates no interaction between the inputs x_4 and x_5 . It is less clear that $d_4(\mathbf{x})$ is independent of x_6 , but the $x_4(\mathbf{x}^{(k)}) \times d_6(\mathbf{x}^{(k)})$ indicates no x_4, x_6 interaction.

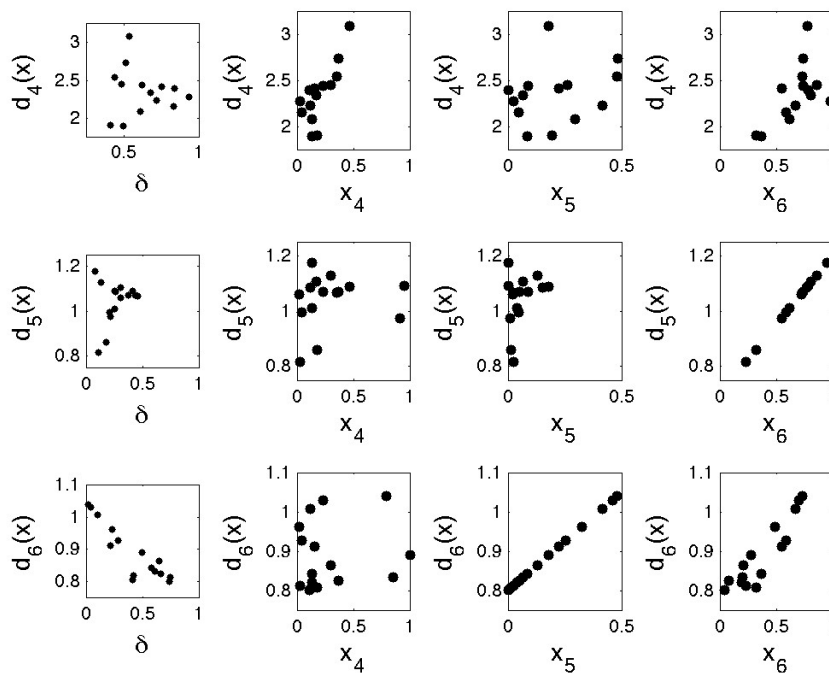


Figure 3: For $i = 4, 5, 6$, the $\delta_i^{(k)} \times d_i(\mathbf{x}^{(k)})$ and $x_j^{(k)} \times d_i(\mathbf{x}^{(k)})$ plots for inputs $j = 4, 5, 6$ for Example 3.1 based on the `SeRStep` OAT design using the $r = 15$ starting points $\mathbf{x}^{(k)}$ in Table 2

Example 3.2 Morris (1991) illustrates the use of OAT designs and EE estimation with the $d = 20$ input polynomial

$$y_m(\mathbf{x}) = \beta_0 + \sum_i^{20} \beta_i w_i + \sum_{i < j}^{20} \beta_{i,j} w_i w_j + \sum_{i < j < l}^{20} \beta_{i,j,l} w_i w_j w_l + \sum_{i < j < l < s}^{20} \beta_{i,j,l,s} w_i w_j w_l w_s \quad (3)$$

having rectangular input region $\mathcal{X} \equiv [0, 1]^{20}$. Here $w_i = 2(1.1x_i/(x_i + 0.1) - \frac{1}{2})$ for $i = 3, 5, 7$, $w_i = 2(x_i - \frac{1}{2})$ otherwise. As in Morris (1991), we selected the large coefficients in (3) to be

$$\begin{aligned}\beta_i &= 20, \quad i = 1, \dots, 10 \\ \beta_{i,j} &= -15, \quad i, j = 1, \dots, 6 \\ \beta_{i,j,l} &= -10, \quad i, j, l = 1, \dots, 5 \\ \beta_{i,j,l,s} &= 5, \quad i, j, l, s = 1, \dots, 4\end{aligned}$$

and the remaining 1st and 2nd order coefficients to be independent draws from the $N(0, 1)$ distribution; all remaining 3rd and 4th order coefficients were set equal to 0.

As illustrated in Figure 4, $y_m(\mathbf{x})$ is non-linear in inputs x_i , $i = 3, 5, 7$ because w_i is non-linear. In addition, inputs x_3 and x_5 are involved in interactions. Inputs x_1, x_2, x_4 and x_6 all have substantial linear effects and are also involved in interactions. On the other hand, inputs x_8, x_9, x_{10} have large linear effects but small interactions. Thus, as Morris (1991) indicates, it should be expected that x_1, \dots, x_{10} have large \bar{d} , while x_8, x_9, x_{10} have small S , and x_1, \dots, x_7 have large S . Finally inputs x_{11}, \dots, x_{20} are inactive and are expected to have both \bar{d} and S close to zero.

In his example, Morris (1991) used a OAT design with a grid width of 1/18, a fixed δ of 2/3, and $r = 4$ randomly selected starting points. For comparison in the hyper-rectangular input region $[0, 1]^{20}$, we constructed a **SeRStep** random δ design with $r = 4$ starting points from a maximin LHD. The left panel of Figure 5 shows the corresponding $\bar{d} \times S$ plot. This plot is qualitatively similar to that of Morris (1991), but there is variability in both the Morris and the **SeRStep** constructions due to the random selection of tours and, for **SeRStep**, the random δ 's. Nevertheless, the plots always separate the active inputs, x_1, \dots, x_{10} , from the inactive inputs, x_{11}, \dots, x_{20} , and identify x_8, x_9 and x_{10} as having strong linear effect (only). The variability issue will be revisited in Section 4.

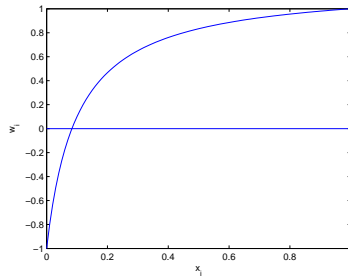


Figure 4: $w_i = 2(1.1x/(x + 0.1) - 0.5)$ versus x .

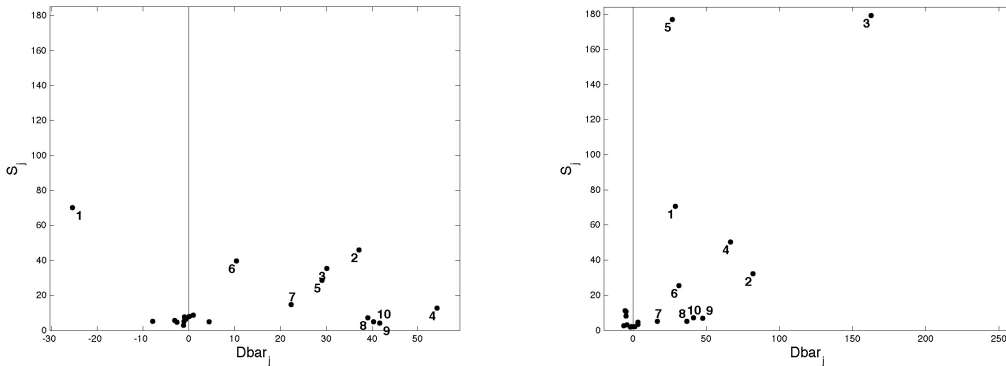


Figure 5: The $\bar{d} \times S$ plots for $y_m(\mathbf{x})$ in Example 3.2 for the **SeRStep** OAT design in a rectangular region $[0, 1]^{20}$ (left panel) and polygonal region (4) (right panel), both using $r = 4$ starting points.

We now impose constraints on the input region with the effect that the activity levels of some of the inputs are modified. The new polygonal input region, which can be written in the form $\mathbf{Ax} \leq \mathbf{b}$ with $\mathbf{L} \leq \mathbf{x} \leq \mathbf{U}$, is taken to be

$$0.2 \leq x_1 + x_5 + x_{11} \leq 1.5, \quad 0 \leq x_3 \leq 0.2, \quad 0.5 \leq x_7 \leq 1, \quad \text{and } 0 \leq x_i \leq 1 \text{ for } i \neq 3, 5, 7. \quad (4)$$

Major differences in EEs are expected for x_3 , x_5 and x_7 because the non-linear function w_i in Figure 4 is applied to different parts of the $[0, 1]$ domain. The constraint $x_3 \in [0.0, 0.2]$ only allows x_3 to take values where w_3 rises rapidly. Thus intuition suggests that x_3 will be more active than it was in the rectangular input problem. Since x_3 has small range, the corresponding δ_3 's have to be small and this leads to greater variability in the d_3 and, consequently, larger S_3 . On the other hand, $x_7 \in [0.5, 0.7]$ is concentrated on “large” values, and w_7 is somewhat flat for these values; thus intuition suggests x_7 will be less active than in the rectangular input problem. The input x_5 is also constrained and is more likely to take values in the middle part of the range which shows the greater gradient variability in Figure 4, so we may expect S_5 to be larger, also.

The **SeRStep** OAT design was applied to $y_m(\mathbf{x})$ with constraints (4) using $r = 4$ starting points determined by **CoNcaD** to form a non-collapsing (approximate) maximin design. The $\bar{d} \times S$ plot, shown in the right panel of Figure 5, indicates the anticipated modified behavior of EEs described in the previous paragraph. With only $r = 4$ EEs, the additional $\delta \times \text{EE}$ and $x \times \text{EE}$ plots are less informative. However, we can see the large variability in d_3 from the $\delta \times d_3$ and $x_3 \times d_3$ plots in Figure 6.

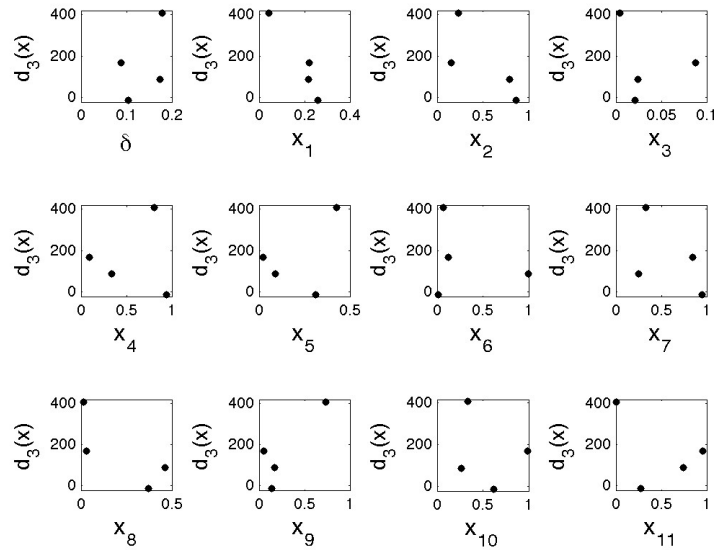


Figure 6: The $\delta \times d_3$ and $x_i \times d_3$ plots, $i = 1, \dots, 11$, for $y_m(\mathbf{x})$ in Example 3.2 with constrained input region (4) for the **SeRStep** OAT design using $r = 4$ starting points.

The examples presented in this section show first that, for applications with rectangular input regions, the **SeRStep** (random δ) OAT design provides $\bar{d} \times S$ plots comparable to those of the Morris OAT design. Secondly, they introduce the $\delta \times \text{EE}$ and $x \times \text{EE}$ plots which, for moderate sized r , allow a more detailed assessment of EE changes for different gradient step lengths than does the $\bar{d} \times S$ plot alone. Finally, the examples illustrate the methodology in two non-rectangular settings.

4 Selection of space-filling tours

When the number, r , of tours is small, the \bar{d}_i and S_i values can vary depending on (i) the selection of starting designs (sets of starting input vectors), (ii) number, r , of starting vectors (and, consequently, number of tours), (iii) selection of $\pm\delta_i$. Below, we investigate the extent of this variability and whether use of space filling *tours*, rather than space-filling *starting points*, is desirable for the identification of active effects.

The function used in the variability study was

$$y(x) = \sum_{j=1}^6 w_j \beta_j + \sum_{i=1}^6 \sum_{j=1}^6 \beta(i, j) w_i w_j \quad (5)$$

which is a modified version of the Morris polynomial model (3) but now with six input variables. Here, w_i is defined below (3), β_i is the i th element of the vector [5, 10, 10, 0.9572, 0.4854, 0.8003], and $\beta(i, j)$ is the $(i, j)^{th}$ element of the matrix

$$\begin{bmatrix} -4.0 & -6.0 & 0.6359 & 0.4064 & 0.2486 & 0.2866 \\ -6.0 & -4.0 & -0.0179 & 0.5640 & 0.3163 & -0.5746 \\ -0.4933 & 0.6051 & 0.3971 & 0.2060 & 0.3215 & -0.2950 \\ 0.4245 & 0.4774 & -0.3677 & 2.0 & -0.1107 & -0.4660 \\ 0.1975 & -0.5108 & -0.1167 & 0.5209 & 0.2320 & -0.6011 \\ -0.4113 & 0.4810 & 0.4249 & 0.4436 & -0.3361 & 0.3306 \end{bmatrix}$$

The values of the parameters show that inputs x_1, x_2 and x_3 have large linear effects, x_1, x_2 and x_4 have large quadratic effects, and x_1, x_2 interact.

Values of \bar{d}_i and S_i , $i = 1, \dots, 6$, were calculated for 5000 SerStep OAT designs constructed from random selections of $r = 4$ starting vectors. The right-most boxplot in the four subfigures of Figure 7 shows the distributions of \bar{d}_i , for $i = 1, 3, 4, 5$. There is considerable variability and the question is whether we can reduce this by selection of a space-filling starting design and well-spaced tours.

Due to the construction of the tours in a OAT design, there is no guarantee that the tours will be well-spaced even if the starting points are. This was recognized by Campolongo et al. (2007) who suggested generating a large number of tours at random and then selecting the best subset of r tours according to a given criterion. They proposed a criterion that maximizes the sum of squared distances between points in different tours; that is, for a given collection of r tours $\mathcal{T} = \{t_1, \dots, t_r\}$, they quantified the spread of these tours by

$$\sqrt{\text{pt-dist}_{1,2}^2 + \dots + \text{pt-dist}_{r-1,r}^2}$$

where the distance between tour t_m and t_ℓ is defined by

$$\text{pt-dist}_{m\ell} = \sum_{u=1}^{k+1} \sum_{v=1}^{k+1} \sqrt{\sum_{j=1}^k [x_j^{(m),u} - x_j^{(\ell),v}]^2} \quad (6)$$

which is sum of the Euclidean distances between every input vector in tour t_m with every input vector in the tour t_ℓ . This tour distance measure does not always make a visually well-spaced selection of tours. For example, we used (6) to select the best $r = 3$ tours out of a random selection of $R = 100$ tours in the (x_5, x_6) constrained region of Example 3.1; the result is shown in the left hand panel of Figure 8. The problem is that four points in two tours are well separated from two points in the third tour and these eight distances outweigh the closeness of the other distances, leading to an unappealing selection.

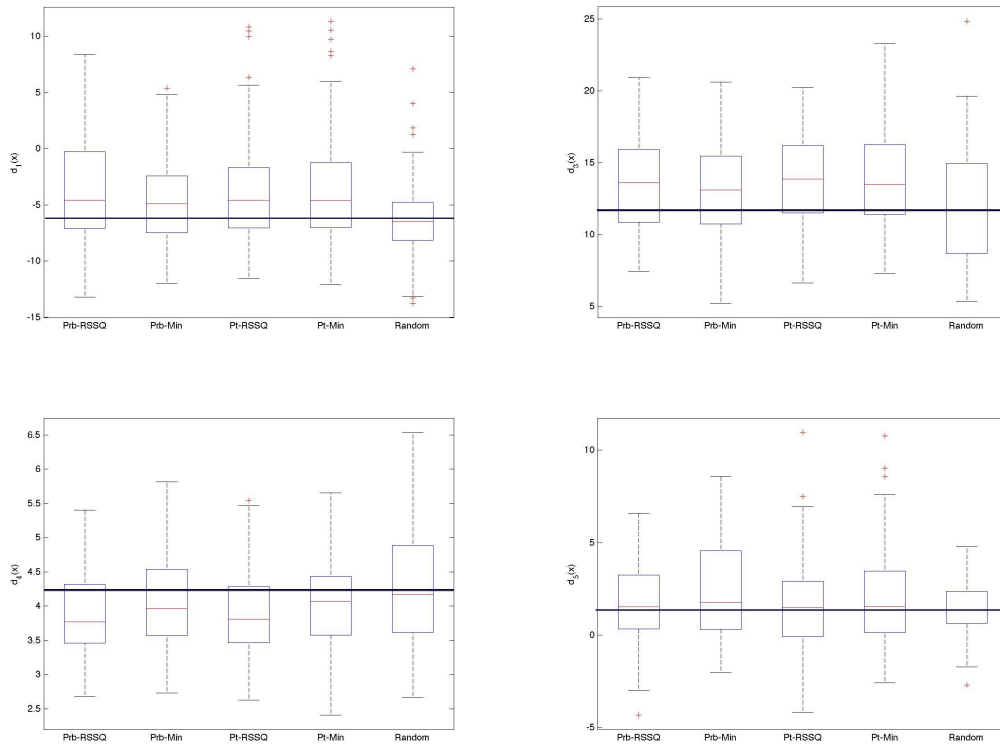


Figure 7: Comparison of observed \bar{d} values computed for inputs 1 (top left), 3 (top right), 4 (bottom left), 5 (bottom right), for model (5), using maximization of (i) root sum of squared probe distances (7), (ii) minimum probe distance (7), (iii) root sum of squared point distances (6), (iv) minimum point distance (6), (v) randomly selected tours.

We investigated an alternative measure that maximizes the minimum distance between corresponding ends of the “probes” in the tours; that is we selected the r tours from R tours that maximizes the minimum value of

$$\text{prb-dist}_{ml} = \sqrt{\sum_{j=1}^k [\min:x_j^{(m)} - \min:x_j^{(\ell)}]^2} + \sqrt{\sum_{j=1}^k [\max:x_j^{(m)} - \max:x_j^{(\ell)}]^2}. \quad (7)$$

From the same 100 tours as before, selection of the $r = 3$ tours that maximize the minimum probe distance (7) is shown in the right hand panel of Figure 8 and this time the tours appear to fill the space.

Figure 7 shows a comparison of the empirical distributions of the \bar{d}_i ($i = 1, 3, 4, 5$) for output function (5) and a set of tours selected under maximization of the (i) sum of squared probe distances (7), (ii) minimum probe distance (7), (iii) sum of squared point distances (6), (iv) minimum point distance (6), (v) randomly selected tours. Values of the mean, $E[\bar{d}_i]$, $i =$

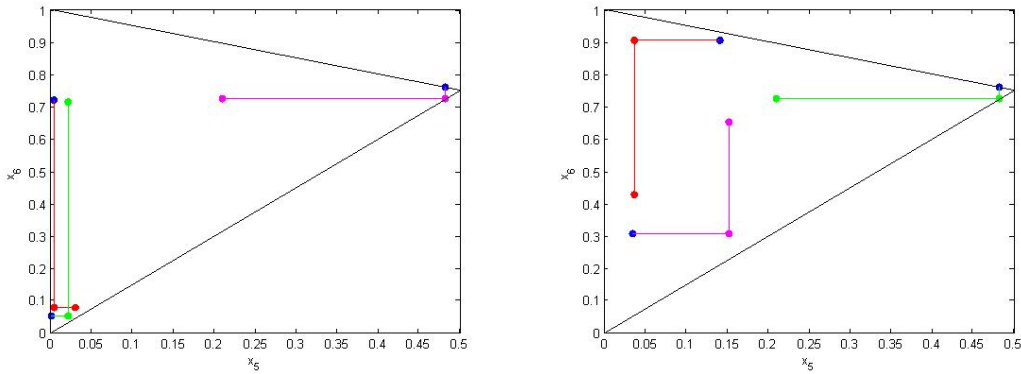


Figure 8: Three tours selected by maximization of (i) sum of squared point distances (6) and (ii) minimum probe distance (7), shown in left and right panels, respectively, for the (x_5, x_6) region of Example 3.1

1, 3, 4, 5, were estimated from 5000 SerStep OAT designs constructed from random selections of $r = 4$ starting vectors and a horizontal line with these values is drawn in each boxplot. The plots show that, in most cases, values of \bar{d}_i larger than $E[d_i]$ tend to be obtained when using space-filling selections of tours. This may be beneficial when seeking active inputs but, otherwise, there seems to be little to be gained by using space filling sets of tours over random starts as far as estimation of \bar{d}_i is concerned, especially as the computational burden is much larger. More work needs to be done to examine the empirical distribution of S_i .

5 Summary and Discussion

This paper has proposed an extension of the OAT design construction procedure of Morris (1991) for estimating elementary effects associated with a deterministic computer simulator. The algorithm, called SerStep, allows calculation of elementary effects in *non-rectangular*, as well as rectangular, input regions. Because the design algorithm adapts the gradient step lengths and directions of the move to the starting points, a *space-filling* set of starting points can be selected to initiate the procedure. The paper introduces $\delta \times \text{EE}$ and $x \times \text{EE}$ plots which can be used to evaluate changes in the output at different ranges and locations of each input.

As do fixed δ OAT designs, SerStep OAT designs allow efficient computation of EEs for high-dimensional input regions. In general, if r elementary effects are determined for each of the d inputs to a computational simulator, the total number of simulator evaluations required by an OAT design is $r(d+1)$. In contrast, a random sample of r starting points for each input plus a δ step to form the gradient would require $2rd$ runs to calculate the same number of

elementary effects. Thus the economy of a OAT design is $(d + 1)/2d$; i.e. approximately $1/2$ for high-dimensional cases (see also Morris 1991).

We have also studied a simplified version of the **SeRStep** OAT design construction (not shown) in which a new, random δ is *fixed* at the start of each tour and used throughout the tour. In addition to being applicable only for rectangular input regions, this variant of **SeRStep** produced $\bar{d} \times S$ plots that tended to provide less definitive separation of active inputs from less active ones. Hence this modification of **SeRStep** is not recommended.

In the Morris (1991) OAT design construction, δ is fixed for each input, so each $d_i(\mathbf{x})$ varies only with \mathbf{x} and not δ which simplifies its interpretation (see $d_4(\mathbf{x})$ in Example 3.1). However, the extra information gained from $\delta \times \text{EE}$ plots is not available in this setting, and the fixed step size could lead to misinterpretations if the function has periodicities that match the size of δ .

Campolongo et al. (2011) argued that radial designs give better performance than the “complete tour designs” studied in this paper and which they call “trajectory-based designs”. In radial designs, instead of a tour, the probes radiate from the starting vector. The gradients $\delta_i^{(k)}$, $i = 1, \dots, d$, are thus all computed with the starting vector $\mathbf{x}^{(k)}$ at one end of the probe ($k = 1, \dots, r$). The input region can be well-explored if the starting vectors are space-filling, but if the starting vectors do not fill the space well, then the radial design is likely to be less good than the trajectory-based designs which give scope to move out across the input space. **SeRStep** can easily be modified to construct radial designs in non-rectangular regions with space-filling starting designs.

Acknowledgments: This research was sponsored, in part, by the National Science Foundation under Agreement DMS-0806134 (The Ohio State University).

References

- Campolongo, F., Cariboni, J. and Saltelli, A. (2007). An effective screening design for sensitivity analysis of large models. *Environmental Modelling & Software* **22**, 1509–1518.
- Campolongo, F., Saltelli, A. and Cariboni, J. (2011). From screening to quantitative sensitivity analysis. a unified approach. *Computer Physics Commun.* **43**, 39–52.
- Draguljić, D., Santner, T. J. and Dean, A. M. (2012). Non-collapsing spacing-filling designs for bounded polygonal regions. *Technometrics* **54**, 169–178.

- Efron, B. and Stein, C. (1981). The jackknife estimate of variance. *Ann. Statist.* **9**, 586–596.
- Liefvendahl, M. and Stocki, R. (2006). A study on algorithms for optimization of latin hypercubes. *J. Statist. Plann. Inf.* **136**, 3231–3247.
- Morris, M. D. (1991). Factorial sampling plans for preliminary computational experiments. *Technometrics* **33**, 161–174.
- Pujol, G. (2009). Simplex-based screening designs for estimating metamodels. *Reliab. Eng. System Safety* **94**, 1156–1160.
- Saltelli, A. and Annoni, P. (2010). How to avoid a perfunctory sensitivity analysis. *Environmental Modelling & Software* **25**, 1508–1517.
- Saltelli, A., Chan, K. and Scott, E. (2000). *Sensitivity Analysis*. John Wiley & Sons, Chichester.
- Sobol', I. M. (1993). Sensitivity analysis for non-linear mathematical models. *Math. Model. Comput. Exp.* **1**, 407–414.
- Stinstra, E., den Hertog, D., Stehouwer, P. and Vestjens, A. (2003). Constrained maximin designs for computer experiments. *Technometrics* **45**(4), 340–346.
- Trosset, M. W. (1999). Approximate maximin distance designs. In *ASA Proceedings, Section on Physical and Engineering Sciences*, pp. 223–227. Am. Statist. Assoc., Alexandria.

Fangfang Sun
Department of Management Science and Engineering
Harbin Institute of Technology
Harbin, Heilongjiang, 150001, China
fangfang@hit.edu.cn

Thomas Santner
Department of Statistics
The Ohio State University
Columbus, OH 43210, USA
santner.1@osu.edu

Angela Dean
Department of Statistics
The Ohio State University
Columbus, OH 43210, USA
dean.9@osu.edu